



A SIMPLE, PHOTOMETRICALLY ACCURATE ALGORITHM FOR DECONVOLUTION OF OPTICAL IMAGES

Author(s): WILLIAM C. KEEL

Source: *Publications of the Astronomical Society of the Pacific*, July 1991, Vol. 103, No. 665 (July 1991), pp. 723-729

Published by: Astronomical Society of the Pacific

Stable URL: <https://www.jstor.org/stable/40651701>

REFERENCES

Linked references are available on JSTOR for this article:

https://www.jstor.org/stable/40651701?seq=1&cid=pdf-reference#references_tab_contents

You may need to log in to JSTOR to access the linked references.

JSTOR is a not-for-profit service that helps scholars, researchers, and students discover, use, and build upon a wide range of content in a trusted digital archive. We use information technology and tools to increase productivity and facilitate new forms of scholarship. For more information about JSTOR, please contact support@jstor.org.

Your use of the JSTOR archive indicates your acceptance of the Terms & Conditions of Use, available at <https://about.jstor.org/terms>



JSTOR

Astronomical Society of the Pacific is collaborating with JSTOR to digitize, preserve and extend access to *Publications of the Astronomical Society of the Pacific*

A SIMPLE, PHOTOMETRICALLY ACCURATE ALGORITHM FOR DECONVOLUTION OF OPTICAL IMAGES

WILLIAM C. KEEL

Department of Physics and Astronomy, University of Alabama, Box 870324, Tuscaloosa, Alabama 35487

Received 1991 March 11, revised 1991 April 29

ABSTRACT

A modified version of the CLEAN deconvolution technique, incorporating a noise model, has been tested on simulated HST data. This straightforward algorithm displays many desirable features for astronomical image reconstruction, as shown by rigorous numerical tests: (1) The photometric scale of the data is preserved accurately. (2) Information on the local noise level due to Poisson statistics in the input data is preserved. (3) It can accommodate a spatially variable point-spread function. Some of these properties are not shared by any widely used deconvolution algorithm. Some considerations of computing speed, and application to ground-based images, are briefly discussed.

Key words: data-handling techniques—CCD images—photometry

1. Introduction

Optical characterization of the Hubble Space Telescope (HST) has brought renewed attention to problems of restoring degraded images in the optical domain. While there has been some work in deconvolving seeing effects from ground-based images (Sharp 1989; Keel 1988; Bendenelli et al. 1990), the point-spread function (PSF) of long exposures has a rather flat peak, so that a very high signal-to-noise ratio is required for a significant gain in resolution. This is not the case for HST images, in which some focus settings yield a sharp image core with of order 10% of the energy on 0.1-arc-second scales. Such images, similar to those produced by a sparsely sampled interferometer, lend themselves well to restoration, and it is of immediate interest to find efficient ways of recovering as much quantitative information as possible from such data.

This paper reports tests of a modified form of the CLEAN algorithm (σ -CLEAN) on simulated HST images, with rigorous tests of the photometric performance of the algorithm. This kind of deconvolution proves to be highly reliable both as to structure and photometric scale down to a quantifiable threshold, depending on the effective scale of the PSF and on the noise level. A straightforward addition (requiring additional memory use but not increased CPU time) can accommodate a spatially variable PSF provided this variation is well understood. Thus, this modification of CLEAN has much to recommend it for restoration and analysis of HST images. A somewhat different version, as previously used by Keel 1988, is in practice more effective on well-sampled ground-based data.

2. The CLEAN Algorithm and a Modification

The CLEAN technique frequently used in processing radio aperture-synthesis data (Högbom 1974; Clark 1980) has an appealing simplicity. It proceeds by locating the peak in a map and subtracting some fraction (the “loop gain”) of its estimated point-source intensity from the map, adding a point source of the same flux to the deconvolved image. This process continues either until some convergence criterion is satisfied or until further iterations would actually diverge in the output estimate. All mathematical operations are linear, the only nonlinear aspect of the algorithm being in the order of selection of the components to be subtracted. While it has been applied to optical data (e.g., Keel 1988), modifications are necessary for efficient work on direct images because of the fundamentally different behavior of noise—noise in an aperture-synthesis map resides in the Fourier domain, but noise in optical images exists in the image domain and, thus, contains Fourier components at all frequencies up to single pixels. Furthermore, the noise varies strongly across a typical direct image, so that residuals due to statistical fluctuations in regions of high surface brightness may be much larger than real and significant features in areas of low surface brightness. Thus, for situations in which deconvolution is desirable, the usual CLEAN algorithm will eventually find noise peaks sharper than the PSF and produce pairs of closely spaced positive and negative components whose amplitude increases with larger numbers of iterations, at the expense of image areas containing physically significant flux (“noise locking”). This problem is most severe in images having a large dynamic range, which are just those for

which deconvolution may yield useful gains.

An effective way of eliminating this behavior uses a noise model for the input image to select the peak which is most significant, not greatest in amplitude. Thus, all 4σ peaks are treated close together and before all 3.5σ ones, and so on. This is the modification to CLEAN described and tested here.

After all so-called CLEAN components have been identified and removed from the original image, the output deconvolved image is produced as the sum of the CLEAN components convolved with a "CLEAN beam" of known size and shape (typically Gaussian) and then added to the residuals from the original image. This guarantees flux conservation and retains the pixel-to-pixel noise useful in assessing the reliability of features in the final image.

The implementation presented here proceeds as follows.

Preprocessing: Major cosmetic flaws (bad columns, radiation events, hot pixels) are removed. So far I have done this by interpolation, but some sort of masking scheme would be superior for HST data since the Wide Field Camera (WFC) PSF contains considerable unresolved structure. The mean background level is subtracted, but information on the Poisson noise introduced by the sky level is carried into the noise model. Saturated areas should be identified, as these may cause problems if located in the region of interest. Again, some sort of masking scheme could be used for saturated areas, though cross correlation might be needed to recover the locations of peaks inside them. The extent of the HST PSF has the amusing result here that a crude restoration of saturated structure is possible in principle from the distant aberrated wings of its image.

Point-spread function: The PSF is normalized within the program. The only important processing steps needed are constructing a version of the PSF with the peak at the center of a pixel and insuring that it goes to zero at the edge of the PSF array. The version of the program here stores the PSF in a simple way, as the normalized intensity assuming the peak is exactly centered in a pixel of the PSF array.

Noise model: This must reflect the noise of the original image (including background). The test version of the code uses the readout noise and inverse gain of a typical chip from the Wide-Field Camera (Griffiths 1985). For a readout noise (1σ) of ρ , sky level of S in analog-to-digital units, intensity I at a given point i,j , and inverse gain of g electrons per ADU, the noise is modeled by

$$\sigma(i,j) = \left(\rho^2 + \frac{S}{g} + \frac{I(i,j)}{g} \right)^{1/2}.$$

In principle, an improved estimator of the noise would use information from the deconvolution to predict the

noise-free input intensity at each point, but this refinement is unlikely to be significant under realistic conditions.

CLEAN iterations: The rate of cleaning is controlled by the loop gain ϵ . For an isolated star image, $\epsilon = 1$ would produce a good estimate of the total flux. However, in the presence of overlapping star images or extended structure, a smaller value is needed to account for light from other points in the image and, more important, so that further iterations will converge. For extended sources, $\epsilon = 0.01$ works well, though values 0.1 or higher may be used for stellar images. If the current residual image (after subtraction of previous CLEAN components) is $R(i,j)$, the next CLEAN component will be taken at the point k,l having the maximum $|R(i,j)/\sigma(i,j)|$; the absolute value operator allows repair of any previous oversubtraction. The noise-model image is unchanged during program execution, since the noise is determined by the original data. A scaled version of the normalized PSF is subtracted, centered at this location. This may be expressed by the substitution

$$R(i,j) \leftarrow R(i,j) - \epsilon R(k,l) \text{PSF}(m,n),$$

where i,j run over regions in which the PSF as shifted is nonzero, and m,n differ from the current i,j by the indices k,l locating the CLEAN component. Finally, the total flux so removed is added as a point source into the CLEAN model $C(i,j)$ of the image:

$$C(k,l) \leftarrow C(k,l) + \epsilon R(k,l).$$

Termination of iterations: The termination criterion has been set using the absolute magnitude of CLEAN components; if such a component (in practice tested every hundredth iteration) exceeds a cutoff value (typically 3) times the minimum so far achieved, divergence due to noise has set in. A fixed number of iterations may be used to prevent the program from running beyond some reasonable point (for example, CLEAN components much smaller than the noise level). Tests on HST WFC images have shown that convergence continues much longer than for simulated data (perhaps due to numerical effects in the realization of simulated noise). The output image is not sensitive to the number of iterations run once the CLEAN components are much smaller than the noise all across the image. This is to be expected since image structure inferred from intensities of single pixels at levels finer than local noise cannot have genuine import for the deconvolved image.

Postprocessing: Both the CLEAN image model $C(i,j)$ and the residual image $R(i,j)$ are saved. The CLEAN image model does not generally contain accurate information on scales as small as a single pixel, either because little modulation is present on such scales in the PSF (for ground-based images) or due to undersampling of the

PSF peak (in WFC images). Thus, following traditional practice in radio astronomy, $C(i,j)$ is convolved with a so-called CLEAN beam before adding to $R(i,j)$. For WFC images, a Gaussian of FWHM 1.5 pixels (0.15 arc second) appears to be appropriate.

3. Demonstration and Tests of σ -CLEAN

Several test images have been processed and the deconvolved images compared in detail to the non-degraded original versions, to demonstrate the linearity and flux conservation of this technique. In general, a modest loop gain (0.01) is most effective. The number of iterations required is of order (number pixels with significant flux/loop gain) when the signal-to-noise ratio is very high, and in practical use much less. To avoid having to specify a number of iterations beforehand, a mild convergence criterion was adopted—when the absolute magnitude of the flux of a component exceeded three times the minimum ever achieved, the routine was stopped. Such a relatively loose criterion was chosen since the magnitude of components chosen by significance fluctuates considerably between iterations, in contrast to the monotonic behavior shown by components in a standard CLEAN. Each test was done in the cases of very high signal-to-noise ratio (to demonstrate the performance of the algorithm itself) and for a realistic level of Poisson noise appropriate to typical data. It is important to note that the same PSF was used for image degradation and deconvolution of the artificial data; I will not discuss here the practical difficulties of generating such a function from the data themselves (see, for example, Stetson 1987).

An exacting test of the ability of the routine to restore images is furnished by a complex extended source, such as a galaxy. The tests shown here use the spiral galaxy NGC 309, whose structure includes a wealth of arm detail and bright knots of a range of sizes. The original image was taken with the Anglo-Australian Telescope in the B pass-band, and block-averaged to simulate the appearance of this large and luminous galaxy as viewed by the HST WFC at $z = 0.6$. The actual WFC PSF was used to construct degraded versions of this image, and restoration was carried out first in the absence of photon noise (to illustrate the numerical accuracy of the program) and then with photon noise corresponding to a long orbital exposure plus varying amounts of sky emission.

These restorations are compared in Figures 1 and 2. Figure 1 compares images (all with the same intensity mapping) of the original data, data at a resolution of 1.5 pixels, as convolved with the WFC PSF, and as restored in the presence of photon noise and different levels of background. Figure 2 shows intensity slices through each of these images, displaying the linearity of the restoration over wide ranges of input intensity, and shows the strong role of sky noise. Trials on actual WFC images (King et al.

1991) show that these simulations are realistic as to the noise behavior, and, in fact, the algorithm will continue to converge for more iterations on real data than on these simulations. Inspection of Figure 2 shows the linear photometric behavior of this algorithm, an important desideratum when quantitative measurements are to be made after deconvolution.

Some tests on artificial star fields have been made. CLEAN does not perform as well as, for example, maximum entropy restoration for point sources very close together (within 2 pixels or so) but may preserve linearity to fainter levels than MEMSYS (as tested by Cohen 1991). Linear algorithms such as this may be particularly useful in providing starting lists of star positions for multistar PSF-fitting techniques such as DAOPHOT.

4. Practical Considerations

The σ -CLEAN algorithm has been run on MicroVAX and Cray X-MP machines. The CPU time per iteration is a strong function of both the size of the region being processed and the extent of the PSF. For very large areas, use of cleaning in a mosaic pattern is most efficient, with overlap of adjacent regions of extent similar to that of the PSF. More elaborate schemes, with parallel processing of various image subsections, might also be envisaged.

For convenience, and to prevent others from having to repeat all my early mistakes in array addressing, a FORTRAN 77 version of the σ -CLEAN algorithm is reproduced here in the Appendix. The working part of the code contains only about 65 lines.

Some improvements in execution speed are possible over the version of the algorithm presented here. For clarity, the data and PSF arrays are addressed here in two dimensions, though storage as appropriately addressed one-dimensional arrays will be faster. Also, certain tests to make sure that the array bounds are not exceeded are done explicitly in the code illustrated, though incorporating them directly into loop indices will allow more efficient vectorization on supercomputers.

A potential advantage of this algorithm is that the PSF need only be defined locally; a whole family of PSF shapes, in principle as many as one per pixel, could be defined and used for deconvolution. Memory requirements would be increased, so that more than 100 or so different PSFs would be prohibitive, but computational time would not be increased.

Finally, a series of tests shows that the σ -CLEAN implementation does not offer such substantial advantages for ground-based images as for HST data, since the peak of the PSF from the ground is relatively flat. The version of CLEAN using smoothing between iterations to suppress statistical noise (Keel 1988) still appears to be more effective in this case.

Rogier Windhorst rekindled my interest in this prob-

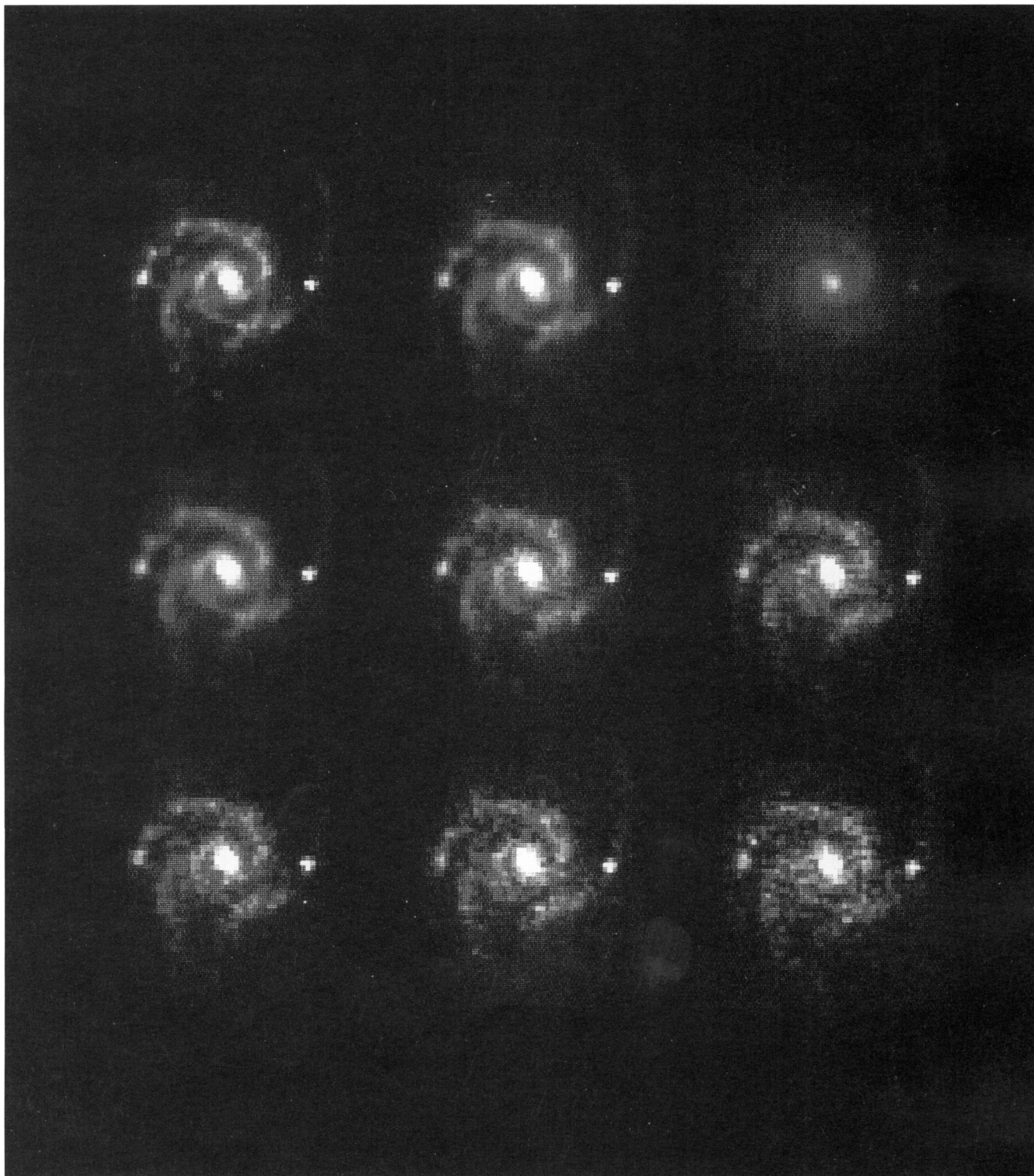


FIG. 1—Test data and deconvolutions in various regimes of noise and background. *Upper left*: original (undersampled) galaxy image. *Top center*: the same test image as seen with a resolution of 1.5 pixels FWHM. This was the target image for restoration, in view of sampling limitations. *Top right*: the image after convolution with the PSF of HST and the Wide-Field Camera. *Center left*: deconvolution of the data blurred by the HST PSF in the limit of high signal-to-noise ratio. This is essentially identical to the target image seen at top center. All deconvolved images have a restoring PSF of FWHM 1.5 pixels (0.15 arc second for the WFC). *Center panel*: the same image with Poisson noise for a long orbital exposure added before deconvolution, assuming negligible background counts. *Center right*: deconvolution including Poisson noise and a background level of 100 ADU per pixel. *Bottom left*: deconvolution for background level of 200 ADU/pixel. *Bottom center*: for background of 400 ADU/pixel. *Bottom right*: for background of 800 ADU/pixel. The intensity scale is the same in each case, to enable direct comparison.

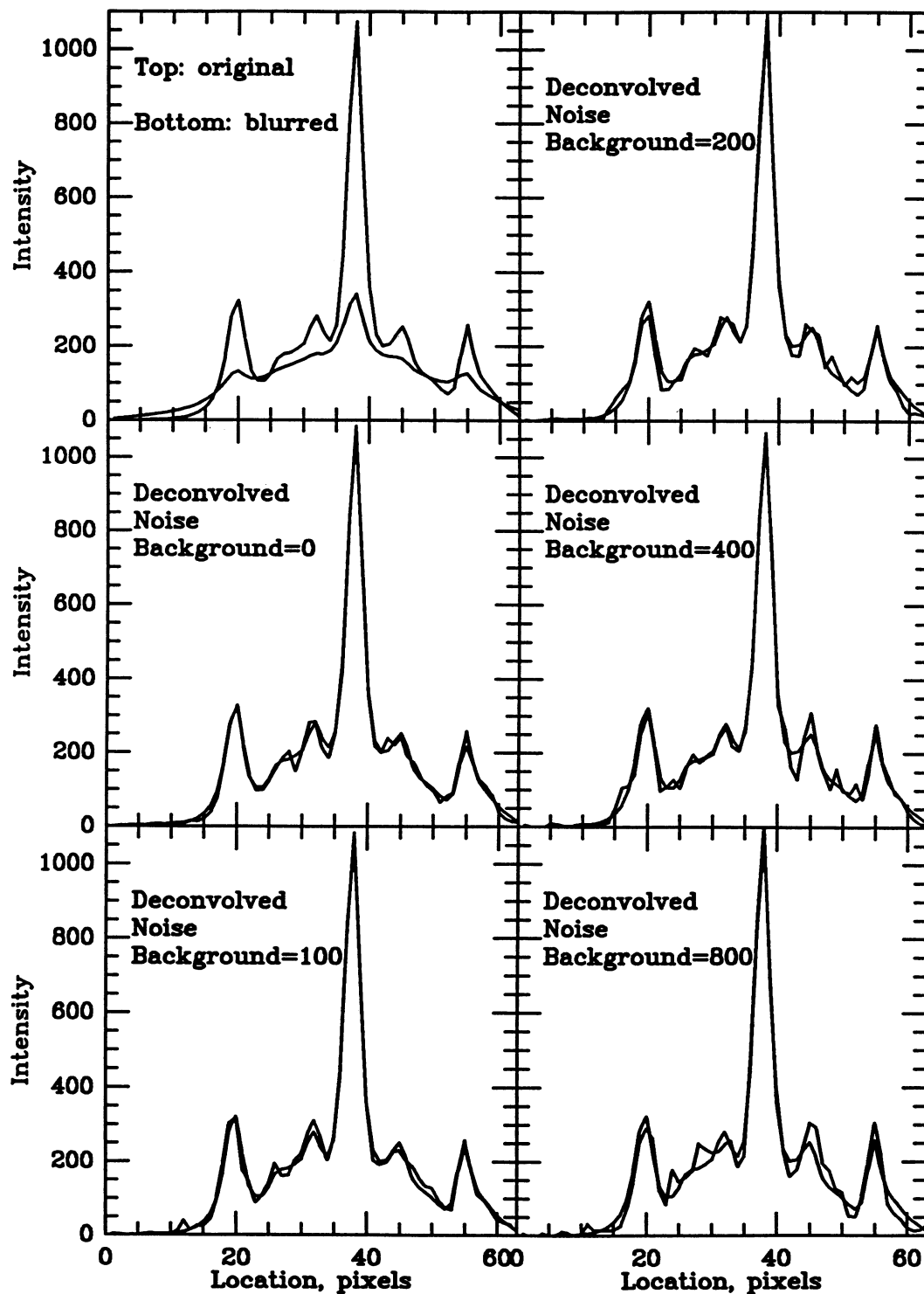


FIG. 2—Horizontal slices through the test data of Figure 1, comparing the original and deconvolved data. The upper-left panel shows the original galaxy image after convolution with a Gaussian beam of 1.5 pixels (or 0.15 arc second for the HST WFC) FWHM at the top, used as a target image to match after deconvolution, and the test data after convolution with the PSF of the HST+WFC, at the bottom. The deconvolved image for the zero-photon-noise case is also plotted and is indistinguishable from the original at this scale. The other panels show the effects of adding Poisson noise due to finite photon flux in the presence of various levels of background light, all given in analog-to-digital units of the WFC. The quality of restoration becomes progressively degraded with increasing background, but the photometric level of the image is preserved as nearly as photon statistics will allow. That is, surface photometry of the deconvolved image will be accurate to the level allowed by statistics of the restored image. For the cases including noise, the ideal original profile is superimposed for comparison.

APPENDIX FORTRAN IMPLEMENTATION OF SIGMA-CLEAN

```

DIMENSION DATA(256,256),CLN(256,256),PSF(80,80)
DIMENSION SIGMA0(256,256),SNR(256,256)
C      SET UP ARRAY DIMENSIONS TO BE READ BY PEAK
C      (CHANGE THESE WHEN DIMENSIONS OF ARRAYS ARE CHANGED)
      NPSF=80
      MPSF=80
      NDATA=256
      MDATA=256
C      set up parameters of noise model
C      ron = effective readout noise in input ADUs
C      (this includes any contribution from subtracted sky noise)
C      gain = electrons/ADU so Poisson noise drops by gain**1/2
      RON=8.
      CCDGAIN=8.
      CCMIN=1.E8
C      PSF RESIDES IN ARRAY PSF, WITH FILLED DIMENSIONS IPSF BY JPSF;
C      ITS DIMENSIONED SIZE IS NPSF BY MPSF
C      INPUT IMAGE (TO BE DECONVOLVED) RESIDES IN ARRAY DATA, WITH FILLED
C      DIMENSIONS NX BY NY; ITS DIMENSIONED SIZE IS NDATA BY MDATA
C      SET UP SIGMA IMAGE
      DO 50 I=1,NX
      DO 45 J=1,NY
      SIGMA0(I,J)=SQRT(RON**2+DATA(I,J)/CCDGAIN)
45      CONTINUE
50      CONTINUE
C      GAIN = LOOP GAIN FOR CLEANING
C      NLOOPS = MAXIMUM ALLOWED ITERATIONS
C      FIND PEAK OF PSF AND ITS POSITION; NORMALIZE
      CALL PEAK (PSF,NPSF,MPSF,IPSF,JPSF,IPSPK,JPSPK,PSFMAX)
      PSUM=0.0
      DO 70 J=1,JPSF
      DO 60 I=1,IPSF
      PSF(I,J)=PSF(I,J)/PSFMAX
      PSUM=PSUM+PSF(I,J)
60      CONTINUE
70      CONTINUE

C      MAIN CLEANING LOOP
      DO 500 NITR=1,NLOOPS
      DO 150 JSIG=1,NY
      DO 140 ISIG=1,NX
      SNR(ISIG,JSIG)=DATA(ISIG,JSIG)/SIGMA0(ISIG,JSIG)
140      CONTINUE
150      CONTINUE
      CALL PEAK (SNR,NDATA,MDATA,NX,NY,IPK,JPk,VMAX)
      VMAX=DATA(IPK,JPk)
      CCFLUX=GAIN*VMAX*PSUM
      CLN(IPK,JPk)=CLN(IPK,JPk)+CCFLUX
      SFLUX=GAIN*VMAX
C      if abs(ccflux) is going up, terminate clean
      IF (ABS(CCFLUX).GT.3.0*CCMIN) GO TO 550
      IF (ABS(CCFLUX).LT.CCMIN) CCMIN=ABS(CCFLUX)
C      IPK,JPk,CCFLUX IS NITR'TH CLEAN COMPONENT
C      SUBTRACT SCALED PSF
      DO 450 J=1,JPSF
      DO 440 I=1,IPSF
      INDEX=IPK-IPSPK+I

```

```

      JINDEX=JPK-JPSPK+J
      IF (JINDEX.LT.1.OR.JINDEX.GT.NY) GO TO 450
      IF (INDEX.LT.1.OR.INDEX.GT.NX) GO TO 440
      DATA(INDEX,JINDEX)=DATA(INDEX,JINDEX)-SFLUX*PSF(I,J)
440    CONTINUE
450    CONTINUE
500    CONTINUE
550    CONTINUE
C      WRITE RESIDUAL MAP (NOW IN ARRAY DATA) TO OUTPUT FILE
C      WRITE CLEAN MODEL (NOW IN ARRAY CLN) TO OUTPUT FILE
      STOP
      END

      SUBROUTINE PEAK (ARRAY,IDIM,JDIM,NX,NY,IPK,JPK,VMAX)
C      FINDS PEAK (ABSOLUTE VALUE) IN ARRAY
C      ARRAY IS IDIM*JDIM, OF WHICH NX*NY IS ACTUALLY FILLED
      DIMENSION ARRAY(IDIM,JDIM)
      VMAX=0.0
      AVMAX=0.0
      DO 100 J=1,NY
        DO 50 I=1,NX
          IF (ABS(ARRAY(I,J)).LT.AVMAX) GO TO 50
          VMAX=ARRAY(I,J)
          AVMAX=ABS(VMAX)
          IPK=I
          JPK=J
50        CONTINUE
100     CONTINUE
      RETURN
      END

```

lem, aided by a number of astronomers who made disparaging remarks about the utility of deconvolution. Dave Block provided the AAT image of NGC 309, and Bob Hanisch provided an HST star image. Peter Stetson gave some extremely thoughtful comments. Jeff Earickson of the Alabama Supercomputer Network and Bill Samayoa of Cray gave valuable advice on improving the computational efficiency of the algorithm. Cray time for some of the tests was made available by the Alabama Supercomputer Network.

REFERENCES

- Bendenelli, O., Parmeggiani, G., Zavatti, F., and Djorgovski, S. 1990, *AJ*, 99, 774
 Clark, B. G. 1980, *A&A*, 83, 377
 Cohen, J. G. 1991, *AJ*, 101, 734
 Griffiths, R. B. 1985, *Wide Field and Planetary Camera Instrument Handbook* (Baltimore, MD, Space Telescope Science Institute)
 Högbom, J. 1974, *A&AS*, 15, 417
 Keel, W. C. 1988, *ApJ*, 329, 532
 King, I., et al. 1991, *AJ*, submitted
 Sharp, N. A. 1989, *ApJ*, 345, L37
 Stetson, P. B. 1987, *PASP*, 99, 191